Research Article

Sustainable Production of Vanillin from Vanillyl Alcohol, a Model Compound of Lignocellulosic Biomass Conversion, via Selective Heterogeneous Catalysis

Daiana Cecilia Latorre
Centro de Investigaciones y Transferencia del Noroeste de la Provincia de Buenos Aires (CITNOBA) – (UNNOBA-UNSAdA-CONICET), Monteagudo 2772 (2700) Pergamino, Buenos Aires, Argentina

IIeana Daniela Lick and Andrea Beatriz Merlo
Centro de Investigación y Desarrollo en Ciencias Aplicadas "Dr. Jorge J. Ronco" (CINDECA) (CCT CONICET-La Plata, UNLP, CICPBA), Universidad Nacional de La Plata, Facultad de Ciencias Exactas, 47 N◦257, 1900 La Plata, Argentina

Daniel Ballesteros-Plata and Enrique Rodríguez-Castellón
Departamento de Química Inorgánica, Cristalografía y Mineralogía, Facultad de Ciencias, Instituto Interuniversitario de Investigación en Biorrefinerías I3B, Universidad de Málaga, 29071 Málaga, España

Mónica Laura Casella
Departamento de Ciencias Básicas y Experimentales, UNNOBA, R. Saenz Peña 456 (6000) Junín, Buenos Aires, Argentina
Centro de Investigación y Desarrollo em Ciencias Aplicadas "Dr. Jorge J. Ronco" (CINDECA) (CCT CONICET-La Plata, UNLP, CICPBA), Universidad Nacional de La Plata, Facultad de Ciencias Exactas, 47 N◦257, 1900 La Plata, Argentina

María Laura Faroppa and Juan José Musci*
Departamento de Ciencias Básicas y Experimentales, UNNOBA, R. Saenz Peña 456 (6000) Junín, Buenos Aires, Argentina
Centro de Investigaciones y Transferencia del Noroeste de la Provincia de Buenos Aires (CITNOBA) – (UNNOBA-UNSAdA-CONICET). Monteagudo 2772 (2700) Pergamino, Buenos Aires, Argentina

* Corresponding author. E-mail: jjmusci@comunidad.unnoba.edu.ar DOI: 10.14416/j.asep.2025.06.005
Received: 16 January 2025; Revised: 10 March 2025; Accepted: 2 April 2025; Published online: 5 June 2025

Abstract
Vanillin, a flavoring agent, is used extensively in the food industry. It is primarily derived from a petroleum derivative through synthetic procedures, though these technologies present certain drawbacks, including the generation of undesired byproducts and a relatively low yield. Furthermore, residual lignocellulosic biomass serves as a renewable source of aromatic compounds with the potential to be used as raw material in the synthesis of vanillin. This would allow the valorization of the residue, resulting in the production of a highly demanded compound for the food industry. To achieve this objective, a heterogeneous Pd catalyst supported on alumina was prepared and its activity was investigated in the oxidation reaction of vanillyl alcohol, a model compound of lignin, to obtain vanillin. The impact of key reaction parameters, including temperature, oxidant concentration, pH of the medium, and solvent, was evaluated. The Pd(1%)/Al_2O_3 catalyst used was capable of achieving 84% conversion and selectivity over 99% towards vanillin under mild conditions after a 3-hour reaction period in an alkaline medium using water as a solvent.

Keywords: Lignocellulosic biomass, Oxidation, Pd/Al_2O_3, Vanillin, Vanillyl alcohol

1 Introduction

Conventional lignocellulosic biomass waste disposal methods, such as combustion and composting, are inadequate in meeting the requirements for carbon neutrality and do not contribute to the development of a sustainable society. This is due to the low efficiency of these methods and the severe pollution they generate [1]. The most contemporary and sustainable treatment strategies for these wastes emphasize their conversion into energy, fuels and bioproducts, thereby contributing to a circular bioeconomy based on lignocellulosic biomass. In recent years, there has been a growing interest in the valorization of lignocellulosic biomass residues and the study of their potential to produce higher added value substances [2]. Lignocellulosic biomass is primarily constituted of three principal components: cellulose, hemicellulose and lignin (Scheme 1).

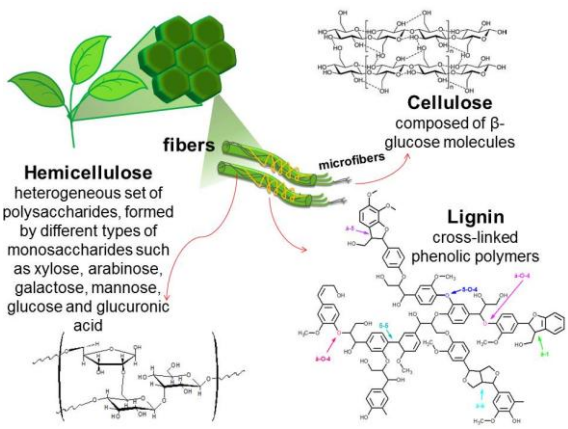

Scheme 1: Representative illustration of the structural composition of lignocellulose and its components.

Lignin constitutes over 20% of the total mass of the biosphere [3]. Moreover, it possesses the dual advantage of being a renewable resource and the sole direct source of renewable aromatic compounds. Additionally, it is an inedible compound, ensuring that it does not compete with the global food supply [4], [5]. In terms of its structure, it can be described as a three-dimensional amorphous polymer, mainly formed of three monomers: synapyl alcohol, coniferyl alcohol and p-coumaryl alcohol. The monomer units are bonded by various C–O and C–C linkages, including β-O-4, β-5, β–β, 5-O-4, α-O-4, 5-5 and β-1, forming a complex matrix with a varying composition [6.]. The specific configuration of this matrix depends on the origin of the biomass and the environmental conditions under which it grows.

Given the inherent complexity and heterogeneity of lignin, most studies investigating lignin valorization employ aromatic monomers that are representative of its structural characteristics [5]. These model compounds simulate the phenolic and non-phenolic functional groups of the propyl side chain of lignin, thus representing the biopolymer while simplifying the reaction network to elucidate the mechanisms involved. Recently, Ali *et al*. published a comprehensive review paper exploring the conversion of the complex structure of lignin, composed of syringyl (S), guaiacyl (G) and p-hydroxyphenyl (H) units, into value-added products [7]. Another interesting monomer found in lignin is vanillyl alcohol (4-hydroxy-3-methoxybenzyl alcohol), which can be used as a model compound in the conversion of lignin to vanillin through oxidative processes.

Vanillin (4-hydroxy-3-methoxybenzaldehyde) is one of the most widely utilized additives in the food industry. Vanillin is added as a flavoring agent in a variety of food products, including ice cream, soft drinks, liquors, candies, confectionery, and baked goods. It is also utilized as a flavor enhancer in coffee and dairy products. Additionally, vanillin possesses antioxidant and antimicrobial properties, making it a valuable component in food products [8]. Furthermore, it serves as a precursor for the synthesis of additional flavoring agents, including ginger and jasmine oil [9]. Additionally, it is used as a ripening agent to enhance the sucrose content in sugarcane [10].

Vanillin has a multitude of applications in the medical, cosmetics, fragrances, nutraceuticals, pharmaceuticals, and fine chemicals industries, where it is employed as a chemical precursor [11], [12]. The global vanillin market size was valued at USD 627.1 million in 2022 and it is anticipated that it will grow at a compound annual growth rate (CAGR) of 7.5% from 2023 to 2030 [13]. Natural vanilla extract represents less than 1% of total vanillin production. At present, the demand for vanillin in the marketplace is approximately 20,000 tons, whereas the natural availability is less than 2,000 tons [14]. While the market for vanillin is comparatively limited in terms of production volume when contrasted with that of other lignin-based compounds, the final product obtained exhibits a notably high added value [15].

Most vanilla extract is obtained through synthetic methods [10]. This phenomenon may be explained by a number of factors, including the fact

that synthetic vanillin is a more cost-effective option. Indeed, the price of synthetic vanillin is approximately one hundred times lower than that of vanillin derived from natural sources (<$15 per kg versus between $1200 and $4000 per kg, approximately) [9]. At present, 85% of vanillin is synthesized from the petrochemical precursor guaiacol by condensation with glyoxylic acid or by the nitrose method (Scheme 2) [16]–[18].

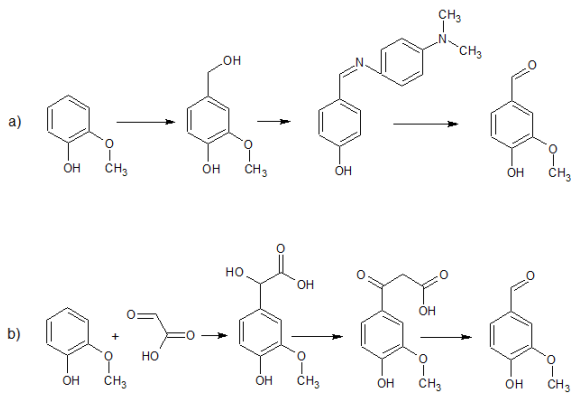

Scheme 2: Traditional methods to obtain vanillin from guaiacol. a) Nitrous method b) glyoxylic method. Adapted from [17].

While these methods yield vanillin with high selectivity, two significant drawbacks must be considered. In the nitrose method, the formation of undesirable byproducts, such as nitrile and p-aminodimethyl aniline, results in a lower product yield. Additionally, the utilization of toxic oxidants, including CuO, MnO_2, and PbO_2, in the glyoxylic method presents a concerning environmental and occupational safety risk [17]. Additionally, certain oxidation reactions necessitate rigorous conditions, such as elevated temperatures and high oxygen pressure [19]. As a consequence, the heterogeneous catalytic oxidation of vanillyl alcohol to vanillin has become a subject that is receiving increased attention.

The heterogeneous catalytic oxidation of vanillyl alcohol is generally carried out via two distinct methodologies. The initial method, designated as "aerobic oxidation", involves the oxidation of vanillyl alcohol by means of high O_2 pressure during hydrothermal processes. The second method involves the oxidation of vanillyl alcohol using H_2O_2 as an oxidant. This method is particularly advantageous as H_2O_2 is a low-cost, easily available and eco-friendly oxidant [20]. Therefore, it is of great importance to identify environmentally friendly alternatives to current vanillin production via the oxidation of vanillyl alcohol using active, selective and reusable catalysts under mild conditions and according to the principles of green chemistry [11].

Many studies show that using supported noble metal catalysts helps to oxidize lignocellulose derivatives. For instance, Wu *et al*., examined Au-Pd catalysts that were supported on phosphate-modified Mg-Al hydrotalcite and activated carbon. The study reported a 52.8% conversion and approximately 50% selectivity, utilizing air as the oxidant in photocatalytic reactions [11]. Wu *et al*., reported using Au nanoparticles and graphene quantum dots as catalysts to oxidise veratryl alcohol to veratryl aldehyde, another model compound used to study lignin transformation pathways [21]. The study yielded interesting results with respect to conversion and selectivity through the modulation of reaction time and pH. It was observed that higher conversions were attained at alkaline pH, while the reaction was directed towards the synthesis of veratric acid rather than veratraldehyde.

In line with these facts, this investigation examines the heterogeneous catalytic oxidation of vanillyl alcohol using H_2O_2 as an oxidizing agent under varying reaction conditions, with the objective of developing a more environmentally sustainable process to produce vanillin than current methods. A Pd/Al_2O_3 catalyst prepared by impregnation was utilized.

2 Materials and Methods

2.1 *Catalyst preparation*

The 1 wt% Pd/Al_2O_3 catalyst was obtained by impregnation with an excess of solution onto commercial alumina (Air Products), which had been previously ground and sieved to a particle size of 60–100 mesh. To achieve this, the required mass of $PdCl_2$ to obtain 1 wt% Pd was dissolved in a 0.01 M HCl solution, resulting in the formation of a water-soluble palladium chloro-complex. The solution was then placed in contact with the γ-Al_2O_3 support for a period of 24 h. After this, the solid was separated from the liquid by decantation and placed in an oven at 105 °C for another 24 h to dry. To reduce the palladium, the dried solid was placed in an Erlenmeyer flask, which was immersed in a water bath at 50 °C. A formaldehyde solution (37 wt%) was added dropwise

until the palladium catalyst turned dark gray. A KOH solution (30 wt%) was then added until a pH value between 9.5 and 10.0 was reached. The final step consisted of subjecting the material to a heating process in an oven maintained at a temperature of 60 °C for a period of 24 h. The remaining chloride on the catalyst was removed by washing with deionized water until no chloride remained, as verified with silver nitrate.

A bimetallic $PdSn_{0.4}/Al_2O_3$ catalyst was prepared via Surface Organometallic Chemistry on Metals (SOMC/M) techniques. To do this, a solution of $SnBu_4$ in n-decane was added to the previously prepared Pd/Al_2O_3 monometallic catalyst. The reaction temperature and time required to achieve a Pd/Sn atomic ratio of 0.4 were established according to previous studies conducted by our research group [22]. 1.199 g of monometallic catalyst and 16 L of $SnBu_4$ dissolved in 15 mL of decane were used for the bimetallic catalyst prepared in this work. The solid was separated from the liquid phase and repeatedly washed with n-heptane under N_2 flow after 4 h of reaction.

The performance of a $PdBi_{0.5}/Al_2O_3$ bimetallic catalyst, prepared by the impregnation method, was also analyzed. In the synthesis procedure, the required quantity of $Bi(NO_3)_3.5H_2O$ was dissolved in a solution of deionized water and HCl (1:1) to achieve an atomic ratio of Bi/Pd = 0.5. The resulting mixture was allowed to stand for 24 h, after which it was dried in an oven at 105°C for a further 24 h. Finally, the solid was reduced by a H_2 stream at 500 °C for 2 h.

2.2 *Support and catalysts characterization*

The textural properties of the support (specific surface area, S_{BET}, and pore volume, Vp) were determined by physical adsorption of N_2 at –196 °C using a Micromeritics ASAP 2020 instrument. The surface morphology was analyzed by scanning electron microscopy (SEM) on an FEI Quanta 200 SEM equipped with an energy dispersive X-ray (EDX) spectrometer (SDD Apollo 40). The concentration of Pd in the catalyst was determined by atomic absorption spectroscopy using a Varian AA 240 spectrophotometer. The metal particle size distribution in the catalyst was determined using a JEOL 100 CX transmission electron microscope (TEM). The samples were ground and dispersed in deionized water by ultrasound. For the determination of the particle size histogram, the mean particle size (d_{VA} mean volume-area diameter) was obtained from Equation (1) by measuring over 200 Pd particles from the micrographs taken directly from the screen using the bright field image.

$$d_{VA} = \frac{\sum n_i d_i^3}{\sum n_i d_i^2} \quad (1)$$

where n_i is the number of particles with a diameter d_i. The surface chemical composition and oxidation state were analyzed by X-ray photoelectron spectroscopy (XPS), employing a PHI Versa Probe II Scanning XPS Microprobe with monochromatic Al Kα (1486.6 eV) X-ray radiation as the excitation source and a charge neutralizer. The pressure within the analysis chamber was kept below 2.0×10^{-6} Pa. High-resolution spectra were recorded at a specified take-off angle of 44° using a multichannel hemispherical electron analyzer operating in the constant-pass energy mode at 29.35 eV. The spectra were referenced to the C 1s signal of adventitious carbon at 284.8 eV. The recorded spectra were analyzed using Multipack software, version 9.6.0.15.

2.3 *Catalytic experiments*

Oxidation reactions were conducted at atmospheric pressure in a 250 mL glass reactor immersed in a thermostatic bath with constant stirring. The reactor was charged with 50 mL of solvent, 1 mmol of vanillyl alcohol (VA), and H_2O_2 as oxidizing agent, and the temperature was increased to the desired value. Once the set temperature was reached, the reaction was initiated by adding 100 mg of catalyst and the reaction was allowed to run for a period of 3 h. Experiments were conducted under a variety of operational conditions to assess the impact of different reaction variables on VA conversion. Each catalytic test was performed in triplicate. Reaction samples were subjected to analysis by ultra-high-performance liquid chromatography (UHPLC) in a DIONEX UltiMate 3000 apparatus, employing a C18 column at 25 °C, with an ultraviolet (UV) detector at 230 nm. The mobile phase consisted of acetonitrile (ACN) 30%-water (H_2O) 70% at a flow rate of 1 mL/min. Identification of the reaction products was performed using a GC/MS apparatus (GCMS QP-2010 ULTRA, Shimadzu, Japan).

3 Results and Discussion

3.1 *Support and catalysts characterization*

The BET surface area and pore volume of the γ-Al_2O_3 support were 216 $m^2\ g^{-1}$ and 0.45 $m^3\ g^{-1}$, respectively. As illustrated in Figure 1(a), the N_2 adsorption-desorption isotherm for γ-Al_2O_3 is classified as type IV(a) according to the IUPAC classification [23]. This type of isotherm is representative of mesoporous materials, for which the adsorption behavior is determined by the interactions between molecules in the condensed state as well as by the interactions between the adsorbate and the adsorbent. In these solids, adsorption occurs in multilayers and hysteresis cycles typical of capillary condensation phenomena are also observed.

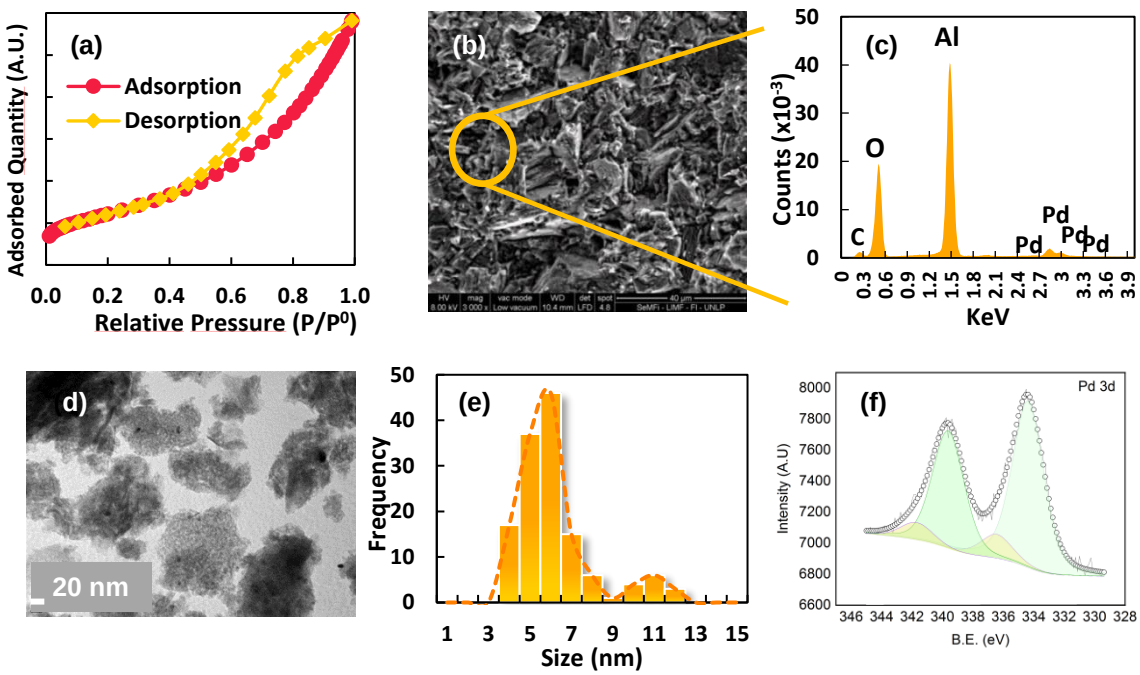

Figure 1: Textural and morphological characteristics of the γ-Al_2O_3 support and Pd/Al_2O_3 catalyst. (a) N_2 adsorption/desorption isotherm of the γ-Al_2O_3 support; (b) and (c) SEM-EDX micrograph of the Pd/Al_2O_3 catalyst; (d) and (e) TEM micrograph with particle size distribution histogram; (f) High resolution Pd 3d core level spectrum of the Pd/Al_2O_3 catalyst

SEM measurements were conducted to elucidate the morphological characteristics of the Pd/Al_2O_3 catalyst and to evaluate the distribution of Pd within the sample. The results of this evaluation are presented in Figure 1(b) and (c). The characteristic porous structure of alumina and a uniform distribution of Pd over the entire catalyst surface was observed, as illustrated by the marked area.

The content of Pd on the catalyst, determined by atomic absorption was 0.98 wt%. This confirmed that the concentration of the metal present on the catalyst was consistent with the nominal content. The transmission electron microscope image (Figure 1(d)) of the Pd/Al_2O_3 catalyst reveals a uniform distribution of metal particles (darker spots) on the support.

The mean particle size (Dva) was determined using data from particle size distribution histograms (Figure 1(e)). A bimodal distribution is observed, with most particles having a mean size of 6.01 nm and a minor contribution from particles with an average value of ca. 11 nm. It has been reported that liquid-phase reduction during the preparation of Pd catalysts often results in broad particle size distributions [24]. In this regard, Lamme *et al*., demonstrated that in the preparation of palladium catalysts supported on carbon nanotubes (Pd/CNT), the reduction process

with sodium borohydride resulted in bimodal particle size distributions, comprising particles of 1 nm and larger than 10 nm in size [25]. The formation of small particles was explained by the adsorption of the metal precursor and the subsequent reduction by the reducing agent. Conversely, the reduction of the precursor species in solution, followed by precipitation, results in the formation of large particles on the support. The dispersion (D) was calculated according to Equation (2) [26] with the d_{VA} value of 6 nm, resulting in a value of 18.52%.

$$D = \frac{6M}{\sigma\rho}\left(\frac{\sum n_i d_i^2}{\sum n_i d_i^3}\right) = 18.52 \approx 19\% \quad (2)$$

where M is the molar mass of Pd, ρ is its density (12.02 g/cm^3), n_i is the number of particles with a diameter di and σ is the area occupied by 1 mol of palladium on the surface (4.77×10^4 m^2 /mol) [27].

X-ray photoelectron spectroscopy (XPS) was employed to examine the surface composition and chemical state of Pd surface species in the Pd/Al_2O_3 catalyst. The spectral regions of the C 1s, Al 2p, O 1s, and Pd 3d core level signals were investigated. The high-resolution Al 2p spectrum exhibits a maximum at approximately 74 eV, while the high-resolution O 1s signal displays its maximum at around 531 eV. The observed binding energies (BE) are characteristic of these elements in the oxidic environment of alumina, which represents the predominant component in the sample. The high-resolution Pd 3*d* core level spectrum (Figure 1(f)) displays the BE of the Pd $3d_{5/2}$ and Pd $3d_{3/2}$ doublet at ca. 335 and 339 eV, respectively. These values correspond to palladium in its metallic state (Pd(0), as previously documented in the literature [28]. In addition, to further investigate the oxidation state of palladium, the Pd $3d_{5/2}$ peak was deconvoluted. The results indicated that although a small contribution of oxidized palladium species appears, it is predominantly in its reduced state on the catalytic surface. The contributions assigned to Pd(0) and Pd(II) appeared at ca. 331–335.5 eV and 335.5–337.6 eV, respectively. Table 1 shows the B.E. of the signals obtained and, in brackets, the percentage contribution of each of these species.

Table 1: Core levels BE (eV) of Pd $3d_{5/2}$, Pd $3d_{3/2}$, O 1*s*, Al 2*p*, for Pd/Al_2O_3 reduced catalyst.

B.E. (eV)				Surface Atomic Ratio
Pd $3d_{5/2}$	**Pd $3d_{3/2}$**	**O 1*s***	**Al 2*p***	**Pd/Al**
Pd(0) 334.4 (87) Pd(II) 336.4 (13)	Pd(0) 339.0	530.9	74.02	0.0048

3.2 *Catalytic tests*

The absence of diffusion limitations was verified by analytical criteria, comparing the maximum transport rates in the physical stages, i.e. diffusion of reactants and/or products at the gas-liquid interface, the liquid-solid interface, and the internal diffusion in particles, with the initial reaction rate. Further details of these studies can be found in the Supplementary Material. In addition, several tests were carried out with different stirring speeds (Figure S1, Supplementary Material), with 700 rpm being a suitable value to ensure a kinetic regime. It was observed that higher stirring speeds resulted in a decrease in the catalytic activity, possibly due to catalyst degradation. Each catalytic test was performed in triplicate. Initially, an experiment was conducted in the absence of a catalyst, thereby confirming that H_2O_2 alone was not capable of oxidizing VA, as no conversion was obtained.

Scheme 3 illustrates the possible reactions involved in the oxidation of vanillyl alcohol (VA) to VN, considering the byproducts identified in the GC/MS analysis.

It has been established that the oxidation of VA by H_2O_2 involves the formation of hydroxyl radicals derived from H_2O_2, which react with the hydroxymethyl group of VA to form vanillin (1). The aldehyde group of vanillin can be subsequently oxidized to give vanillic acid (2) [29]. Vanillin can undergo oxidation to 2-methoxy-1,4-benzenediol (3) via the Dakin oxidation reaction [30]. The observation of this product was limited to trace quantities in the reactions of the present study involving high concentrations of H_2O_2 in acetonitrile. Additionally, 1,4–2 methoxybenzoquinone (4) was identified in trace amounts. This finding aligns with previous observations by other authors [31], [32].

Initial studies were performed using acetonitrile as the solvent because it was reported in the literature to be a suitable medium for this reaction [31], [33]–[35].

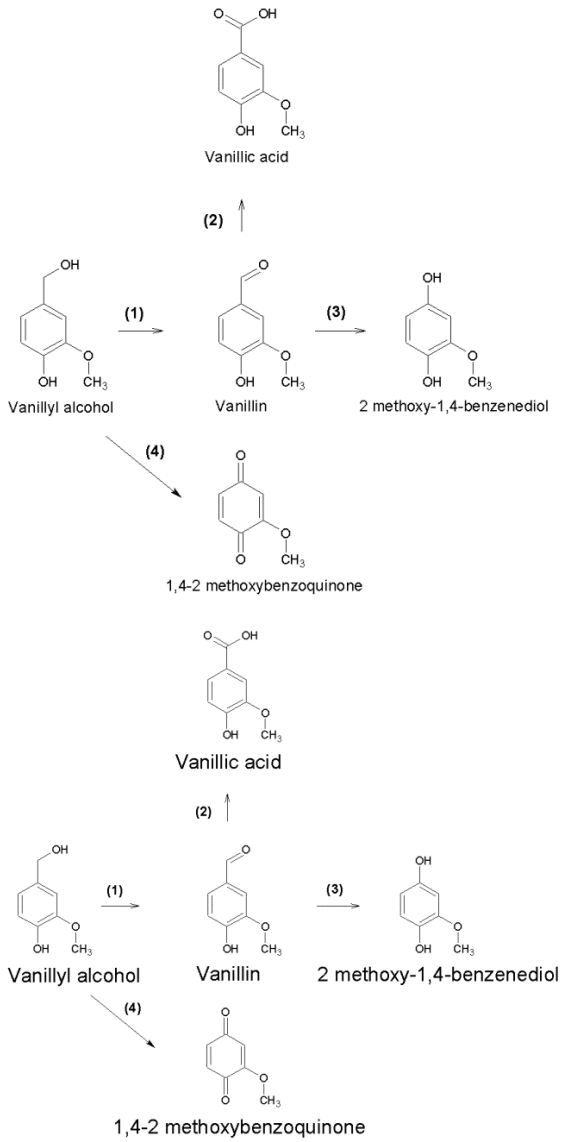

Scheme 3: Possible products derived from VA oxidation.

The results obtained with different concentrations of H_2O_2 and acetonitrile as solvent are shown in Figure 2(a). It was determined that the conversion remained between 30 and 40% when the amount of oxidant was increased from 2 to 10 mmol, indicating that the amount of hydroxyl radicals present was sufficient to ensure the oxidizing capacity of the medium. After 3 hours of reaction, the selectivity to vanillin reached its maximum (17%) at 8 mmol H_2O_2 and decreased drastically with the subsequent increase in oxidant concentration. This was a result of the undesired oxidation or degradation of vanillin, which favored the formation of some by-products (2-methoxy-1,4-benzenediol and 1,4-2-methoxybenzoquinone). The same behavior with respect to the dependence of conversion and selectivity to vanillin as a function of H_2O_2 concentration was previously observed by Elamathi *et al.* [31]. The authors employed a FeMCM-41 (100) catalyst at 60 °C and observed that the conversion of VA increased gradually from 85 to 95% as the molar ratio of H_2O_2 to VA increased from 1 to 5. Simultaneously, the selectivity to vanillin exhibited a marked decline, dropping from 82 to 13% as the concentration of the oxidant increased.

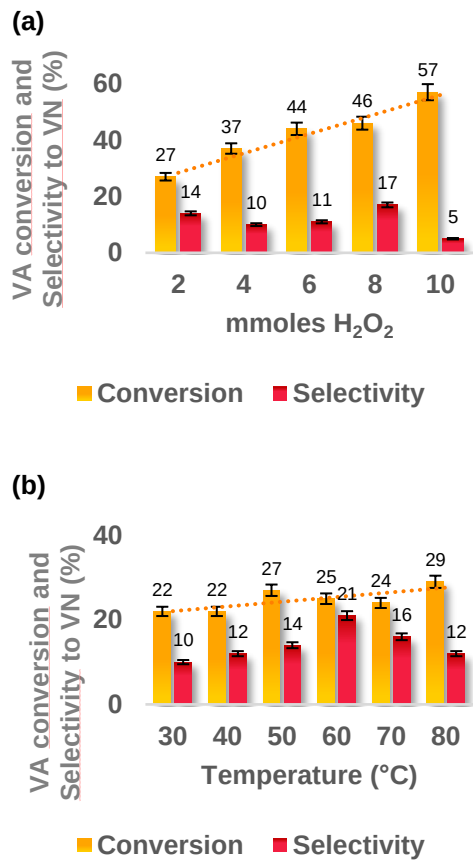

Figure 2: Conversion (%) of VA and Selectivity (%) to VN: (a) as a function of H_2O_2 concentration and (b) as a function of temperature. Reaction conditions: catalyst loading = 100 mg, VA = 1 mmol, solvent = 50 mL final vol., t = 3 h, stirring speed: 700 rpm. T = 50 °C (Figure 2(a)), H_2O_2 = 2 mmol (Figure 2(b)).

Regarding the effect of temperature (Figure 2(b)), it was observed that conversion increased from 22 to 27% as the temperature increased from 30 to 50 °C. No significant increase in conversion was observed with further increases in this variable. Higher temperatures favored vanillin degradation to other compounds, explaining the decrease in selectivity above 60 °C (where maximum selectivity to vanillin was observed).

The influence of the solvent and the pH of the reaction medium were also investigated. Inspired by the literature, a series of experiments were conducted. These experiments included tests that were performed without pH control [29]–[31], [34]–[41] and tests in which the reaction medium was alkaline [17], [33]. Initially, experiments were carried out using acetonitrile as a solvent because it has been reported to enhance the VA oxidation reaction by promoting the formation of active radical species [42]. Subsequently, the reaction was studied in a strong alkaline medium by adding 4 mmol NaOH. However, when using acetonitrile, it was not possible to obtain an adequate reaction mixture and distribution of the catalyst in the reaction medium, and the reagent could not be solubilized. Therefore, other solvents were tested (Table 2), keeping in mind that polar solvents favor the reaction. Moderate results were obtained in isopropanol (ISO) with 33% conversion of VA and 47% selectivity to vanillin. Precipitate formation was observed in the reaction medium, indicating that higher conversion was not achieved due to the low solubility of the reagent in the medium. Conversely, the reaction in the aqueous medium (W) achieved 84% VA conversion with a selectivity towards VN over 99%. It has been proposed that an alkaline medium stabilizes the aldehyde group of VN and prevents further oxidation. This explains the high selectivity of the reaction towards vanillin [43]. Furthermore, under these conditions, the formation of the perhydroxide radical from peroxide would be favored, since it is a more reactive species than the hydroxyl radical [44]. This is also an explanation for the increased activity observed in this case.

Table 2: Conversion and Selectivity to VN for oxidation of AV in different solvents in an alkaline medium.

Catalyst	Solvent	X%[a]	S_{VN}%
Pd/α-Al_2O_3	ACN	-	-
	ISO	33	47
	W	84	<99

α % conversion at 180 min reaction.

The results obtained in the present work are very promising. Although in many cases several authors have achieved very good results, with high conversions and/or selectivities, the reaction conditions do not always follow the principles of green chemistry. The development of an environmentally friendly technology for obtaining vanillin from lignocellulosic biomass must take into account: using low- or non-toxic reagents, avoiding or using harmless solvents and separating agents, minimizing energy requirements, operating at or near ambient temperature and pressure, and selecting substances that minimize chemical accidents [18]. Also, the type of catalytic material used must be relatively inexpensive and easy to produce, as well as active and selective. In the literature, there are several works on VA oxidation using different active phases and operating conditions. For a direct comparison with the results obtained in this work, a summary of those works using H_2O_2 as oxidant is presented below, as well as some results using O_2.

As can be seen in Table 3, besides the results presented in this paper (entries 1 and 2), only one reference (entry 5) uses water as a solvent. This work describes the use of a Co_3O_4 catalyst assisted by low frequency ultrasound irradiation at 75 °C for 15 min. In this sono-Fenton assisted oxidation, a VA conversion of 38% and a selectivity to VN of 50% were obtained [30]. It is worth mentioning that the temperature used by the authors was 75 °C, which is higher than the one used in our case. Regarding this operating parameter, the results found ranged from 50 °C (entry 8) to 140 °C (entry 13). In the first case, Saberi *et al*. [34] reported the use of an iron oxide-based magnetic material (Fe_2O_3/Al-SBA-15) with interesting results (99% conversion and 88% selectivity), despite using a higher oxidant to VA ratio. In the case of entry 13, Palli *et al*. [39] reported the use of a $Ce_{0.8}Fe_{0.2}O_2$ catalyst that achieved 91% conversion and 99% selectivity in acetonitrile at 140 °C using O_2 as oxidant.

Concerning the heterogeneous noble metal catalysts, it has been documented that Pt (entry 14) and Au-Pd (entry 15) were used, yielding conversions of 32% and 53%, respectively. In contrast, higher yields were achieved when Pd was employed as the active metal (entries 16 and 17). With regard to the operating conditions, in all cases O_2 was used as an oxidant, and different solvents were employed instead of water.

It can be said that the results reported in the present work are very promising and meet the above-

mentioned requirements of green chemistry by using a harmless solvent such as water and mild operating conditions (temperature of 50 °C and atmospheric pressure). This would result in enhanced energy efficiency, reduced waste, and the utilization of clean processes.

Table 3: Catalytic performances of catalysts for the oxidation of VA to VN.

Entry	Catalyst	Conditions	T (°C)	t (h)	X_{VA} (%)	S_{VN}	Yield (%)	Ref.
1	Pd(1%)/γ - Al_2O_3	1 mmol VA; 2 mmol H_2O_2; 50 mL water; 0.1g catalyst	50	3	15	95	14.25	this work
2	Pd(1%)/γ - Al_2O_3	1 mmol VA; 2 mmol H_2O_2; 4 mmol NaOH; 50 mL water; 0.1g catalyst	50	3	84	<99	83.16	this work
3	$CoTiO_3$	1 mmol VA; 2 mmol H_2O_2; 2 mmol NaOH; 25 mL isopropanol; 0.1g catalyst	85	5	99	99.8	90.8	[33]
4	Cu-Ti composite oxides	1 mmol VA; 3 mmol H_2O_2; 20 mL acetonitrile; 0.05g catalyst	85	1	66	71	46.9	[36]
5	Co_3O_4	1.3 mmol VA; 2 mmol H_2O_2; 4 mL water; 0.004g catalyst; 20 kHz ultrasound	75	0.25	38	50	19	[30]
6	FeMCM-41	1.0 mmol VA, 1 mmol H_2O_2, 30 mL acetonitrile, 0,2 g catalyst	60	0.5	85	82	69.7	[31]
7	Carbon-supported cobalt nanocomposite	2 mmol VA, 0,6 mmol H_2O_2, 50 mL acetonitrile, 0.1 g catalyst	85	1	50	95	47.5	[29]
8	Fe_2O_3/Al-SBA-15[(10)]	5.2 mmol VA, 20 mmol H_2O_2, 50 mL acetonitrile, 0.1 g catalyst	50	2	99	88	88.1	[34]
9	$CuO/MgAl_2O_4$	5 mmol VA, 20 mmol H_2O_2, 8 mL acetonitrile, 0.1 g catalyst	90	8	81	100	81	[35]
10	$CuO/MgFe_2O_4$	5 mmol VA, 20 mmol H_2O_2, 8 mL acetonitrile, 0.1 g catalyst	90	8	64	100	64	[35]
11	$Cu_{0.4}Co_{0.6}Fe_2O_4$@PC	1 mmol VA, 1 mmol H_2O_2, 40 mL acetonitrile, 0.075 g catalyst	80	0.66	96	81	77.8	[37]
12	$Cu_{0.1}Ce_{0.9}O_{2-\delta}$	200 mg VA, O_2 (atm. pressure), 10 mL N, n-dimethyl formamide; 0.050 g catalyst	130	12	95	100	95	[38]
13	$Ce_{0.8}Fe_{0.2}O_2$	300 mg VA; O_2 (20 bar); 20 mL acetonitrile; 100 mg catalyst	140	5	91	99	90.1	[39]
14	Pt/CuClP	1g VA; air (20 bar); 30 mL t-butanol; 50 mg catalyst	150	10	32	76	24.3	[40]
15	Au–Pd bimetallic nanoparticles on phosphorylated hydrotalcite	0.2 mmol VA; 3 mL dioxane; 50 mg catalyst; exposed to visible-light irradiation emitted by a 300 W Xe arc lamp	25	24	53	50	26.5	[11]
15	Pd/C	1 mmol VA; O_2 (5 bar); 10 mL p-xylene; 20 mg catalyst	120	9	83	100	83	[41]
16	0.1Sn-Pd/C	1 mmol VA; O_2 (3 bar); 10 mL p-xylene; 15 mg catalyst	120	6	100	100	100	[41]

The introduction of a second non-precious metal promoter onto the Pd active sites represents a well-established methodology to modify the catalytic characteristics of the monometallic-based catalyst [45], [46].

In that sense, the influence of adding a second metal as a promoter to the Pd(1%)/Al_2O_3 catalyst was

subsequently investigated to determine if the catalytic performance could even be improved. Based on previous studies carried out in our research group, the performance of a bimetallic $PdBi_{0.5}/Al_2O_3$ catalyst prepared by the successive impregnations method and a bimetallic $PdSn_{0.4}/Al_2O_3$ catalyst prepared by Surface Organometallic Chemistry on Metals (SOMC/M) techniques have been evaluated. This last technique allows a bimetallic catalyst with well-defined properties (particle size and surface composition) to be obtained under mild reaction conditions. These bimetallic catalysts have been extensively studied in our working group and they have shown good catalytic performance in oxidation reactions using H_2O_2 as oxidant [47], [48].

The preparation of the latter catalyst by these techniques can be described as a two-step process. First, the system is heated to 120 °C in an H_2 atmosphere; this allows the formation of an organobimetallic compound where the organic groups are anchored to the metallic surface. In the second step, the catalyst is reduced in a stream of H_2 at 500 °C for 2 h. The bimetallic phase is obtained by releasing all the organic fragments in this step. The reactions can be represented as follows:

$$Pd/Al_2O_3 + ySnBu_4 + \frac{xy}{2}H_2 \rightarrow Pd\left(SnBu_{4-x}\right)_y/Al_2O_3 + xyBuH$$

$$Pd\left(SnBu_{4-x}\right)_y/Al_2O_3 + \frac{(4-x)y}{2}H_2 \rightarrow PdSn_y/Al_2O_3 + (4-x)yBuH$$

The reaction between $SnBu_4$ and Pd/Al_2O_3 was followed by GC, measuring the variation of the organometallic compound concentration in the impregnation solution. It was found that the initial concentration of the $SnBu_4$ solution does not affect the maximum amount of Sn incorporated, and the saturation value depends only on the temperature. It was also found that with this technique, the Sn is selectively deposited on the Pd particles and not on the support. Table 4 shows the reaction conditions used in the preparation of the bimetallic catalyst, including the measured initial and final concentrations of $SnBu_4$.

As depicted in Figure 3, the $PdBi_{0.5}/Al_2O_3$ catalyst showed a conversion of 38% and very low selectivity to VN, less than 5%, when tested in an alkaline medium. Under the same alkaline conditions, the $PdSn_{0.4}/Al_2O_3$ catalyst showed a conversion of 83% with a selectivity to VN of 92%.

Table 4: Preparation of PdSn catalyst and amount of tin fixed (measured as Sn/Ru ratio).

Catalyst	T (°C)[(1)]	M (g)[(2)]	Reaction Time (h)	C_i (mmol L^{-1})[(3)]	C_f (mmol L^{-1})[(3)]	mmol Sn fixed	mmol Pd	Sn/Pd[(4)]
Pd $Sn_{0.4}/\gamma$-Al_2O_3	120	1.199	4	3.2	0.17	0.046	0.113	0.40

[(1)] Reaction Temperature.
[(2)] Mass of monometallic catalyst used.
[(3)] $SnBu_4$ concentration (C_i = initial concentration and C_f = final concentration).
[(4)] Atomic Relation.

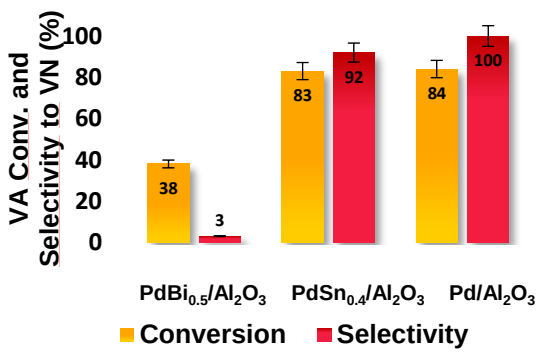

Figure 3: Conversion (%) of VA and Selectivity (%) to VN using $PdBi_{0.5}/Al_2O_3$, $PdSn_{0.4}/Al_2O_3$ and Pd/Al_2O_3 catalysts. Reaction conditions: catalyst loading = 100 mg, VA = 1 mmol, solvent (water) = 50 mL final vol., H_2O_2 = 2 mmol, T = 50 °C, t = 3h, stirring speed: 700 rpm.

Sun *et al.* [37] studied the oxidation of vanillyl alcohol using O_2 as oxidant and p-xylene as solvent, at 120 °C and with Pd/C and PdM/C catalysts (M = Mn, Co, Cu, Zn, and Bi, metal loading = 0.1 wt%). They observed that Sn promoted the conversion of vanillyl alcohol, with an increase of approximately 45% from 69 to 100%. Conversely, the introduction of Bi, Cu, Mn, Co and Zn resulted in a reduction in alcohol conversion, with values decreasing to between 21 and 54%.

To investigate the reusability of the Pd/Al_2O_3, a sample of the catalyst was repeatedly used in the oxidation of vanillyl alcohol. After each cycle, the catalyst was separated from the reaction mixture by filtration. The catalyst was then dried at 105 °C for 2 h. As shown in Figure 4, no significant drop in vanillyl alcohol conversion was observed until the catalyst was reused three times. On the third use, the conversion

drops probably due to catalyst lixiviation, as can be concluded by observing the presence of Pd in the reaction medium by atomic absorption studies. A notable aspect is that the selectivity to VN maintained high values during all reuses.

The powder catalyst was destroyed during the process, so it could not be used for further testing. However, this does not invalidate the results, which show the catalyst's activity. In order to implement an industrial application of the process, it would be interesting to explore the possibility of developing a structured catalytic system to enhance its mechanical resistance.

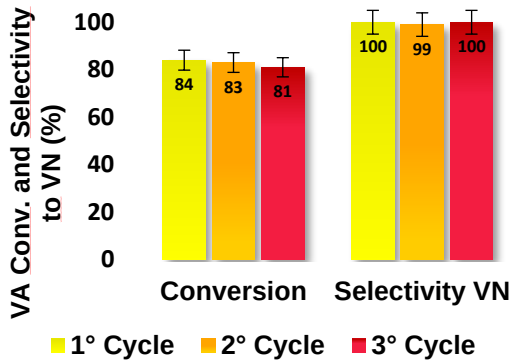

Figure 4: Reutilization study for the Pd/Al_2O_3 catalyst. Reaction conditions: catalyst loading = 100 mg, VA=1 mmol, solvent (water) = 50 mL final vol., H_2O_2 = 2 mmol, T = 50 °C, t = 3h, stirring speed: 700rpm.

4 Conclusions

The oxidation of vanillyl alcohol was studied using a $Pd(1\%)/Al_2O_3$ catalyst and H_2O_2 as an oxidizing agent. It was possible to obtain a high conversion of alcohol (84%) with selectivity over 99% to vanillin under mild pressure and temperature conditions, using water as a solvent in an alkaline medium. Additionally, the catalyst was reused three times without any significant loss of activity, consistently exhibiting a high selectivity towards vanillin. However, it was not feasible to use the catalyst for further testing. The addition of a second metal did not introduce noticeable improvements in the catalytic performance. Moreover, in the case of PdBi, there was a considerable decrease both in the VA conversion and in the selectivity to vanillin.

The methodology represents an interesting alternative for the preparation of vanillin from lignocellulosic biomass by means of an environmentally friendly process using mild reaction conditions and water as solvent.

The catalytic results obtained in the laboratory are promising. Nevertheless, it is challenging to achieve further improvements in the performance of the catalyst in terms of its stability. In this regard, the development of a structured catalytic system to enhance the mechanical strength will be considered. Additionally, the activity, selectivity and stability of the catalytic system will be evaluated in relation to its direct application with material derived from lignocellulosic biomass.

Acknowledgement

This work has been carried out with the financial support received from UNNOBA (SIB Project 1664/2022). The authors are grateful to Eng. H.P. Bideberripe for carrying out the gas chromatography/mass spectrometry tests. D.B.P and E.R.C. thank to Spanish Ministry of Science and Innovation, project PID2021-126235OB-C32 funded by MCIN/ AEI/10.13039/501100011033/ and FEDER funds, and project TED2021-130756B-C31 funded by MCIN/AEI/10.13039/501100011033 and by "ERDF A way of making Europe" by the European Union Next Generation EU/PRTR.

Author contributions

D.C.L.: investigation, methodology, writing an original draft; M.L.F.: investigation, writing an original draft; A.B.M.: investigation, methodology, data analysis, writing an original draft; D.B.P.: data analysis, data curation; E.R.C.: writing—reviewing and editing, data analysis, funding acquisition, project administration; I.D.L.: research design, data analysis, data curation, writing—reviewing and editing; M.L.C.: conceptualization, research design, writing—reviewing and editing, funding acquisition, project administration; J.J.M.: conceptualization, methodology, data curation, writing— reviewing and editing. All authors have read and agreed to the published version of the manuscript.

Conflicts of Interest

The authors declare no conflict of interest.

References

[1] K. Wang and J. W. Tester, "Sustainable management of unavoidable biomass wastes," *Green Energy and Resources*, vol. 1, no. 1, Mar 2023, Art. no. 100005, doi: 10.1016/j.gerr.2023.100005.

[2] J. Zakzeski, P. C. Bruijnincx, A. L. Jongerius, and B. M. Weckhuysen, "The catalytic valorization of lignin for the production of renewable chemicals," *Chemical reviews*, vol. 110, no. 6, pp. 3552–3599, Mar. 2010, doi. 10.1021/cr900354u.

[3] S. Areeya, E. J. Panakkal, M. Sriariyanun, T. Kangsadan, A. Tawai, S. Amornraksa, U. W. Hartley, and P. Yasurin, "A review on chemical pretreatment of lignocellulosic biomass for the production of bioproducts: Mechanisms, challenges and applications," *Applied Science and Engineering Progress*, vol. 16, no. 3, pp. 6767, 2023, doi: 10.14416/j.asep.2023.02.008.

[4] M. Oregui-Bengoechea, I. Agirre, A. Iriondo, A. Lopez-Urionabarrenechea, J. M. Requies, I. Agirrezabal-Telleria, K. Bizkarra, V. L. Barrio, and J. F. Cambra, "Topics in current chemistry collections," in *Lignin Chemistry*, L. Serrano, R. Luque, and B. F. Sels, Eds. Berlin: Springer, pp. 197–271, 2020.

[5] R. Behling, S. Valange, and G. Chatel, "Heterogeneous catalytic oxidation for lignin valorization into valuable chemicals: What results? What limitations? What trends?," *Green Chemistry*, vol. 18, no. 7, pp. 1839–1854, Jan. 2016, doi: 10.1039/C5GC03061G.

[6] M. N. F. Norrrahim, R. A. Ilyas, N. M. Nurazzi, M. S. A. Rani, M. S. N. Atikah, and S. S. Shazleen, "Chemical pretreatment of lignocellulosic biomass for the production of bioproducts: An overview," *Applied Science and Engineering Progress*, vol. 14, no. 4, pp. 588–605, 2021, doi: 10.14416/j.asep.2021.07.004.

[7] S. Ali, A. Rani, M. A. Dar, M. M. Qaisrani, M. Noman, K. Yoganathan, M. Asad, A. Berhanu, M. Barwant, and D. Zhu, "Recent advances in characterization and valorization of lignin and its value-added products: Challenges and future perspectives," *Biomass*, vol. 4, no. 3, pp. 947–977, Sep. 2024, doi: 10.3390/biomass4030053.

[8] R. Rao and G. A. Ravishankar, "Vanilla flavour: production by conventional and biotechnological routes," *Journal of the Science of Food and Agriculture*, vol. 80, no. 3, pp. 289–304, Jul. 2000, doi: 10.1002/1097-0010(200002)80:3<289::AID-JSFA543>3.0.CO;2-2.

[9] G. A. Martău, L. F. Călinoiu, and D. C. Vodnar, "Bio-vanillin: Towards a sustainable industrial production," *Trends in Food Science & Technology*, vol. 109, pp. 579–592, Mar. 2021, doi: 10.1016/j.tifs.2021.01.059.

[10] M. Fache, B. Boutevin, and S. Caillol, "Vanillin production from lignin and its use as a renewable chemical," *ACS Sustainable Chemistry & Engineering*, vol. 4, no. 1, pp. 35–46, Dec. 2016, doi: 10.1021/acssuschemeng.5b01344.

[11] M. Wu, J. H. Pang, P. P. Song, J. J. Peng, F. Xu, Q. Li, and X. M. Zhang, "Visible light-driven oxidation of vanillyl alcohol in air with Au-Pd bimetallic nanoparticles on phosphorylated hydrotalcite," *New Journal of Chemistry*, vol. 43, no. 4, pp. 1964–1971, Jan. 2019, doi: 10.1039/C8NJ05477K.

[12] M. Fache, E. Darroman, V. Besse, R. Auvergne, S. Caillol, and B. Boutevin, "Vanillin, a promising biobased building-block for monomer synthesis," *Green Chemistry*, vol. 16, no. 4, pp. 1987–1998, Feb. 2014, doi: 10.1039/C3GC42613K.

[13] G. V. Research. "Vanillin market size & trends." grandviewresearch.com. https://www.grandviewresearch.com/industry-analysis/vanillin-market (accessed Feb. 12, 2025).

[14] Y. Liu, L. Sun, Y. X. Huo, and S. Guo, "Strategies for improving the production of bio-based vanillin," *Microbial Cell Factories*, vol. 22, no. 147 pp. 1–11, Aug. 2023, doi: 10.1186/s12934-023-02144-9.

[15] R. J. A. Gosselink, "Lignin as a renewable aromatic resource for the chemical industry," Ph.D. thesis, Wageningen University, Netherlands, 2011.

[16] M. M. Bomgardner. "The problem with vanilla," *Chemical & Engineering News*, vol. 94, no. 36, pp. 38–42, Sep. 2016.

[17] A. Jha and C. V. Rode, "Highly selective liquid-phase aerobic oxidation of vanillyl alcohol to vanillin on cobalt oxide (Co_3O_4) nanoparticles," *New Journal of Chemistry*, vol. 37, no. 9, pp. 2669–2674. Jun. 2013, doi: 10.1039/C3NJ00508A.

[18] R. Ciriminna, A. Fidalgo, F. Meneguzzo, F. Parrino, L. M. Ilharco, and M. Pagliaro, "Vanillin: The case for greener production driven by sustainability megatrend," *Chemistry*

Open, vol. 8, no. 6, pp. 660–667, May. 2019, doi: 10.1002/open.201900083.

[19] W. Hou, N. A. Dehm, and R. W. J. Scott, "Alcohol oxidations in aqueous solutions using Au, Pd, and bimetallic AuPd nanoparticle catalysts," *Journal of Catalysis*, vol. 253, no. 1, pp. 22–27, Jan. 2008, doi: 10.1016/j.jcat.2007.10.025.

[20] J.-Y. Lin, H.-K. Lai, and K.-Y. A. Lin, "Rapid microwave-hydrothermal conversion of lignin model compounds to value-added products via catalytic oxidation using metal organic frameworks," *Chemical Paper*, vol. 72, pp. 2315–2325, Mar. 2018, doi: 10.1007/s11696-018-0452-4.

[21] X. Wu, S. Guo, and J. Zhang, "Selective oxidation of veratryl alcohol with composites of Au nanoparticles and graphene quantum dots as catalysts," *Chemical Communications*, vol. 51, no. 29, pp. 6318–6321, Apr. 2015, doi: 10.1039/c5cc00061k.

[22] G. F. Santori, M. L. Casella, G. J. Siri, H. R. Adúriz, and O. A. Ferretti, "Hydrogenation of crotonaldehyde on Pt/SiO_2 catalysts modified with tin added via surface organometallic chemistry on metals techniques," *Applied Catalysis A: General*, vol. 197, no. 1, pp. 141–149, Apr. 2000, doi: 10.1016/S0926-860X(99)00548-7.

[23] M. Thommes, K. Kaneko, A. V. Neimark, J. P. Olivier, F. Rodríguez-Reinoso, J. Rouquerol, and K. S. W. Sing, "Physisorption of gases, with special reference to the evaluation of surface area and pore size distribution," *Pure and Applied Chemistry*, vol. 87, no. 9–10, pp. 1051–1069, 2015, doi: 10.1515/pac-2014-1117.

[24] W. S. Lamme, O. van der Heijden, N. A. Krans, E. Nöllen, N. Mager, S. Hermans, J. Zečević, and K. P. de Jong, "Origin and prevention of broad particle size distributions in carbon-supported palladium catalysts prepared by liquid-phase reduction," *Journal of Catalysis*, vol. 375, pp. 448–455, Jul. 2019, doi: 10.1016/j.jcat.2019.06.034.

[25] W. S. Lamme, J. Zečević, and K. P. de Jong, "Influence of metal deposition and activation method on the structure and performance of carbon nanotube supported palladium catalysts," *ChemCatChem*, vol. 10, no. 7, pp. 1552–1555, Jan. 2018, doi 10.1002/cctc.201701991.

[26] J. Yang, V. Tschamber, D. Habermacher, F. Garin, and P. Gilot, "Effect of sintering on the catalytic activity of a Pt based catalyst for CO oxidation: Experiments and modelling," *Applied Catalysis B: Environmental*, vol. 83, no. 3–4, pp. 229–239, Sep. 2008, doi: 10.1016/j.apcatb.2008.02.018.

[27] G. Bergeret and P. Gallezot, "Particle size and dispersion measurements," in *Handbook of Heterogeneous Catalysis*, 2nd ed., vol. 2, G. Erltl, H. Knözinger, F. Schüth, and J. Weitkamp, Eds. Weinheim, Germany: Wiley-VCH, pp. 738–765, 2008, doi. 10.1002/9783527610044.hetcat0038.

[28] K. Pattamakomsan, E. Ehret, F. Morfin, P. Gélin, Y. Jugnet, S. Prakash, J. C. Bertolini, J. Panpranot, and F. J. Cadete Santos Aires, "Selective hydrogenation of 1,3-butadiene over Pd and Pd–Sn catalysts supported on different phases of alumina," *Catalysis Today*, vol. 164, no. 1, pp. 28–33, Apr. 2011, doi: 10.1016/j.cattod.2010.10.013.

[29] K. Y. A. Lin, H. K. Lai, and Z. Y. Chen, "Selective generation of vanillin from catalytic oxidation of a lignin model compound using ZIF-derived carbon-supported cobalt nanocomposite," *Journal of the Taiwan Institute of Chemical Engineers*, vol. 78, pp. 337–343, Sep. 2017, doi: 10.1016/j.jtice.2017.06.029.

[30] R. Behling, G. Chatel, and S. Valange, "Sonochemical oxidation of vanillyl alcohol to vanillin in the presence of a cobalt oxide catalyst under mild conditions," *Ultrasonics Sonochemistry*, vol. 36, pp. 27–35, May 2017, doi: 10.1016/j.ultsonch.2016.11.015.

[31] P. Elamathi, M. K. Kolli, and G. Chandrasekar, "Catalytic oxidation of vanillyl alcohol using FeMCM-41 nanoporous tubular reactor," *International Journal of Nanoscience*, vol. 17, no. 01–02, 2018, Art. no. 1760010, doi: 10.1142/S0219581X17600109.

[32] A. Jha, D. Mhamane, A. Suryawanshi, S. M. Joshi, P. Shaikh, N. Biradar, S. Ogale, and C.V. Rode, "Triple nanocomposites of $CoMn_2O_4$, Co_3O_4 and reduced graphene oxide for oxidation of aromatic alcohols," *Catalysis Science & Technology*, vol. 4, no. 6, pp. 1771–1778, Mar. 2014, doi: 10.1039/C3CY01025B.

[33] M. Shilpy, M. A. Ehsan, T. H. Ali, S. B. Abd Hamid, and M. E. Ali, "Performance of cobalt titanate towards H_2O_2 based catalytic oxidation of lignin model compound," *RSC advances*, vol. 5, no. 97, pp. 79644–79653, Sep. 2015, doi: 10.1039/C5RA14227J.

[34] F. Saberi, D. Rodríguez-Padrón, E. Doustkhah, S. Ostovar, A. Franco, H. R. Shaterian, and R. Luque, "Mechanochemically modified aluminosilicates for efficient oxidation of vanillyl alcohol," *Catalysis Communications*, vol. 118, pp. 65–69, Jan. 2019, doi: 10.1016/j.catcom.2018.09.017.

[35] B. Rahmanivahid, M. Pinilla-de Dios, M. Haghighi, and R. Luque "Mechanochemical synthesis of $CuO/MgAl_2O_4$ and $MgFe_2O_4$ spinels for vanillin production from isoeugenol and vanillyl alcohol," *Molecules*, vol. 24, no. 14, Jul. 2019, Art. no. 2597, doi: 10.3390/molecules 24142597.

[36] S. Saha and S. B. Abd Hamid, "$CuZrO_3$ nanoparticles catalyst in aerobic oxidation of vanillyl alcohol," *RSC advances*, vol. 7, no. 16, pp. 9914–9925, Jan 2017, doi: 10.1039/c6ra26370d.

[37] M. Cui, L. Dong, Z. Shen, T. Guo, W. Zhao, C. L.iang, X. Liu, D. Wang, F. Wang, Z. Jiang, and S. Fu, "Preparation of porous carbon supported Co element doping spinel copper ferrite for the catalytic oxidation of vanillyl alcohol," *Applied Catalysis A: General*, vol. 664, Aug. 2023, Art. 119325, doi: 10.1016/j.apcata.2023.119325.

[38] S. Nazeer, S. Palli, Y. Kamma, M. K. Palnati, B. M. Reddy, and T. Venkateshwar Rao, "Mesoporous copper-cerium mixed oxide catalysts for aerobic oxidation of vanillyl alcohol," *Catalysts*, vol. 13, no. 7, Jun 2023, Art. 1058, doi: 10.3390/catal13071058.

[39] S. Palli, Y. Kamma, S. Nazeer, B. M. Reddy, and T. Venkateshwar Rao. "Oxidation of vanillyl alcohol to vanillin over nanostructured cerium–iron mixed oxide catalyst with molecular oxygen," *Research on Chemical Intermediates*, vol. 48, no 11, pp. 4579–4599, Sep. 2022, doi: 10.1007/s11164-022-04827-1.

[40] C. S. Hinde, D. Ansovini, P. P. Wells, G. Collins, S. V. Aswegen, J. D. Holmes, T. S. A. Hor, and R. Raja, "Elucidating structure–property relationships in the design of metal nanoparticle catalysts for the activation of molecular oxygen," *ACS Catalysis*, vol. 5, no. 6, pp. 3807–3816, May. 2015, doi: 10.1021/acscatal.5b00481.

[41] W. Sun, S. Wu, Y. Lu, Y. Wang, Q. Cao, and W. Fang, "Effective control of particle size and electron density of Pd/C and Sn-Pd/C nanocatalysts for vanillin production via base-free oxidation," *ACS Catalysis*, vol. 10, no. 14, pp. 7699–7709, Jul. 2020, doi: 10.1021/acscatal.0c01849.

[42] A. Al-Hunaiti, A. Ghazzy, N. Sweidan, Q. Mohaidat, I. Bsoul, S. Mahmood, and T. Hussein, "Nano-Magnetic $NiFe_2O_4$ and its photocatalytic oxidation of vanillyl alcohol—synthesis, characterization, and application in the valorization of lignin," *Nanomaterials*, vol. 11, no. 4, Apr. 2021, Art. no. 1010, doi: 10.3390/nano11041010.

[43] C. S. McCallum, W. Wang, W. J. Doran, W. G. Forsythe, M. D. Garrett, C. Hardacre, J. J. Leahy, K. Morgan, D.S. Shin, and G.N. Sheldrake, "Life cycle thinking case study for catalytic wet air oxidation of lignin in bamboo biomass for vanillin production," *Green Chemistry*, vol. 23, no. 4, pp. 1847–1860, Feb. 2021, doi: 10.1039/D0GC03685D.

[44] L. J. Csányi, L. Nagy, M. Galbács, and I. Horváth, "Alkali-Induced generation of superoxide and hydroxyl radicals from aqueous hydrogen peroxide solution," *Zeitschrift für Physikalische Chemie*, vol. 138, no. 1, pp. 107–116, Jul. 1983, doi: 10.1524/zpch.1983.138.1.107.

[45] H. Wang, L. Jiao, L. Zheng, Q. Fang, Y. Qin, X. Luo, X. Wei, L. Hu, W. Gu, J. Wen, and C. Zhu, "PdBi single-atom alloy aerogels for efficient ethanol oxidation," *Advanced Functional Materials*, vol. 31, no. 38, Jul. 2021, Art. 2103465, doi: 10.1002/adfm.202103465.

[46] N. Xaba, R. M. Modibedi, M. K. Mathe, and L. E. Khotseng, "Pd, PdSn, PdBi, and PdBiSn nanostructured thin films for the electro-oxidation of ethanol in alkaline media," *Electrocatalysis*, vol. 10, no. 11, pp. 332–341, Feb. 2019, doi: 10.1007/s12678-019-0511-9.

[47] M. L. Faroppa, "Valorización de biomasa. Desarrollo de catalizadores heterogeneos para la oxidación del glicerol crudo obtenido en el proceso de producción de biodiesel," Ph.D. thesis, Universidad Nacional del Noroeste de la Provincia de Buenos Aires, Argentina, 2023.

[48] M. L. Faroppa, M. E. Chiosso, J. J. Musci, M. A. Ocsachoque, A. B. Merlo, and M. L. Casella, "Oxidation of glycerol in base-free aqueous solution using carbon-supported Pt and PtSn catalyst," *Catalysts*, vol. 13, Jul. 2023, Art. no. 1071, doi: 10.3390/catal13071071.

Supporting Information

1 Controlling stages of oxidation reactions

For liquid-phase oxidation reactions, mass transfer processes can affect the reaction rate and must be absent to ensure that the reaction is governed by kinetic rather than by mass transfer parameters, i.e. the rate of the physical processes is greater than the rate of the chemical reactions.

In the case of three-phase catalytic systems, the transport processes of reactants from the phase in which they are fed into the reactor to the contact with the catalyst where they react and then, the reverse steps followed by the products are as follows:

- Gas/liquid mass transfer;
- Diffusion of reactants and products in the liquid phase to and from the catalyst particle (external diffusion);
- Diffusion of reactants and products inside the catalyst pores (internal diffusion).

2 Characteristics of Reactions in Heterogeneous Catalysis

For a gaseous reactant to be catalytically converted into products in a three-phase system, a given sequence must generally occur. It first needs to be transferred from the gas phase to the liquid phase and then, to the catalytic interface. Once it has reached the active site it can adsorb on it or react with another adsorbed reagent (Eley-Rideal-type reactions). The product must then be desorbed and transferred from the interface to the liquid phase.

The transport steps can be classified as follows, considering a catalyst with a porous structure:

1) Dissolution of the gaseous reagent in the liquid medium.
2) Diffusion of the dissolved reactants towards the catalyst particle (external diffusion).
3) Diffusion of the reactants into the catalyst pores (internal diffusion).
4) Adsorption of the reactants on the catalyst surface.
5) Chemical reaction on the active surface of the catalyst.
6) Desorption of the product.
7) Diffusion of the products out of the catalyst particle.
8) Diffusion of the products from the particle into the liquid stream.

The diffusion steps are physical processes, while the other steps are chemical ones.

3 Diffusional Limitations

Experimental or analytical criteria can be used to identify the existence of diffusional limitations. In the first case, the variation of the reaction rate or any other experimental parameter, such as the stirring rate, is studied. In the second case, the reaction rate is compared with the maximum transport rates in the physical steps by calculating transfer coefficients and diffusivities.

3.1 *Experimental criteria*

To experimentally ensure that there were no mass transfer limitations, tests were conducted in which the stirring speed was varied between 400 and 800 rpm at 50 °C with 172 µL of 136 vol. H_2O_2 and 50 mL of solvent, using 100 mg of the monometallic catalyst Pd/C and 150 mg (1 mmol) of Vanillyl Alcohol (VA) as substrate. As illustrated in Figure S1, the initial reaction rates (ri) for each stirring speed are depicted, calculated from the slopes of the conversion vs. time curves (at 10% conversion). It is evident that at stirring speeds below approximately 600 rpm, (ri) exhibits a decline, indicative of mass transfer limitations. Consequently, a speed of 700 rpm was selected for the subsequent tests.

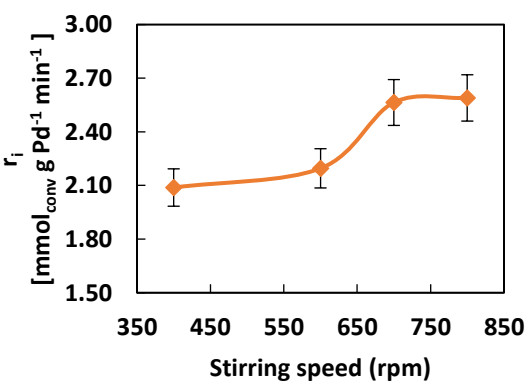

Figure S1: Initial reaction rate vs Stirring speed. Reaction conditions: catalyst loading = 100 mg, VA = 1 mmol, solvent = 50 mL final vol., t = 3 h, T = 50 °C, H_2O_2 = 2 mmol.

3.2 *Analytical criteria*

When analytical criteria are used, the initial reaction rate is compared with the maximum transport rates in the physical steps. In the case of the oxidation reaction with hydrogen peroxide, in the liquid phase, the diffusion of reactants and/or products at the gas/liquid interface, at the liquid/solid interface, and inside the particle is evaluated. The expressions used for the calculation of the different coefficients are given below.

3.2.1 Diffusional limitations at the gas/liquid interface

For this case, we started from the assumption that hydrogen peroxide can decompose releasing O_2 that acts as an oxidizing agent, whose diffusion limitation constitutes the most unfavorable case among the possible oxidizing agents that may be present in the reaction medium. Thus, to ensure that there is no resistance to the transport of O_2, the gaseous reactant released from H_2O_2, at the gas/liquid interface, the following relationship must be fulfilled Equation (S1):

$$\alpha_1 = \frac{(r_i)_{obs}}{k_L \cdot a_G \cdot C_{O_2}} \leq 0.1 \quad \text{(S1)}$$

Where:

$(r_i)_{obs}$: initial reaction rate obtained experimentally;

k_L : matter transfer coefficient at the gas-liquidinterface;

a_G : interfacial area per unit volume of reactor;

C_{O_2} : O_2 concentration in the liquid phase calculated from the initial amount of H_2O_2.

The criterion states that if the observed reaction rate is less than 10% of the value of the maximum gas/liquid matter transfer rate, then the transport process is much faster than the observed chemical reaction, thus not limiting the overall process.

For the calculation of the coefficient $k_L.a_G$ various correlations determined by several authors can be used. One of them is that proposed by Meille *et al.* who studied the determination of the coefficient $k_L.a_G$ in laboratory tank reactors, magnetically stirred and without the use of baffles, whose volumes were between 25 and 300 cm^3 (Gas/liquid mass transfer in small laboratory batch reactors: Comparison of methods). In their work, they obtained a linear relationship between the coefficient and the stirring speed. Considering the 150 cm^3 capacity reactor, which is the one that most resembles the one used in this work, the correlation to be used is shown in Equation (S2):

$$k_l \cdot a_G = 1.14 \cdot 10^{-4} \cdot N^{2.98} \quad \text{(S2)}$$

For a stirring speed of N=700 rpm= 11.67 s^{-1}, a coefficient of $k_L.a_G = 0.1723\ s^{-1}$ is obtained.

The reaction conditions used were 50 °C with 172 µL of 136 vol. H_2O_2 and 50 mL of solvent, using 100 mg of the monometallic catalyst Pd/C and 150 mg (1 mmol) of Vanillyl Alcohol (VA) as substrate. From the conversion curve, the initial reaction rate at 10% conversion was calculated and then, the $\propto_{(1\text{-}O2)}$ criterion was applied. The results in Table S1 show that under the working conditions, there are no limitations for O_2 transport at the gas/liquid interface and within the reaction volume. Since it is satisfied that $\propto_{(1\text{-}O2)} < 0.1$, it can be said that the reaction rate does not exceed 10% of the transport rate of the reactant.

Table S1: Calculation of parameters at the gas/liquid interface.

Parameter	$k_l.a_G$ [1/s]	C_{O2} [mol/L]	$(r_i)_{obs}$ [mol/L.s]	$\propto_1$
Value	0.1723	0.021	4.27×10^{-3}	0.01

3.2.2 Diffusional limitations at the liquid/solid interface

To determine that there is no resistance to the transfer of the reagents at the liquid/solid interface, the criterion taken is the same as that employed for the gas/liquid interface. For both reactants (O_2 and VA), it must be fulfilled that the ratio between the reaction rate and the rate of transport of matter must be less than 10%. That is, if Equation (S3) applies:

$$\alpha_2 = \frac{(r_i)_{obs}}{k_C \cdot a_C \cdot m_c \cdot C_i} \leq 0.1 \quad \text{(S3)}$$

$(r_i)_{obs}$: initial reaction rate obtained experimentally;

k_C : matter transfer coefficient at the liquid/solid interface;

m_c : catalyst mass;

C_i : reagent concentration in liquid phase;

a_C : external area of the catalyst per unit mass of catalyst, calculated by Equation (S4):

$$a_C = \frac{6}{d_p \cdot \rho_p} \quad \text{(S4)}$$

d_p : catalyst particle diameter; $d_p \approx$ 200 microns = 0,02 cm

ρ_p : density of catalyst particles; $\rho_p \approx$ 540 kg/m^3 = 0,54 g/cm^3

For the calculation of the transfer coefficient k_C, the expression proposed by Martínez was used (Transferencia de materia en tanques agitados: Disolución de sólidos puros) for suspended particles in spherical stirred tank reactors, Equation (S5):

$$\frac{k_C \cdot d_p}{D_M} = 66.5 \cdot \left(\frac{N \cdot d_l^2}{\mu_M}\right)^{0.23} \cdot \left(\frac{\mu_M \cdot d_l^2}{\rho_M \cdot D_M}\right)^{1/3} \cdot \left(\frac{d_{TM}}{h}\right)^{0.104} \quad \text{(S5)}$$

D_M : molecular diffusivity of the reactants in the reaction mixture;

d_l : stirrer diameter = 2 cm;

d_T : inside diameter of the tank = 8 cm

h : height of liquid level = 4 cm

ρ_M : reaction mixture density; $\rho_M \approx$ 1 g/cm^3

μ_M : dynamic viscosity of reaction mixture; μ_M = 0,00466 g/(cm.s)

Diffusion coefficients were obtained by correlation of the Wilke-Chang model (Correlation of diffusion coefficients in dilute solutions). Thus, with the values of kc and the rest of the data presented below, the values of $\propto_2$ for the two reagents are calculated and presented in Table S2.

a_C = 555, 55 cm^2/g

m_c = 0,100 g

Table S2: Calculation of parameters at the liquid/solid interface.

Parameter	$k_{c\text{-}O2}$ [cm/s]	$k_{c\text{-}VA}$ [cm/s]	$\propto_{2-O2}$	$\propto_{2-VA}$
Value	1.261	0.159	2.92×10^{-4}	2.41×10^{-3}

3.2.3 Intraparticle diffusional limitations

The Weisz-Prater criterion was used for both reagents to check whether there are resistances to matter transfer within the catalyst particle. According to this criterion, the limitations to matter transport are negligible if Equation (S6) is fulfilled:

$$\Phi = \frac{(r_i)_{obs} \cdot L^2}{D_i^e \cdot C_i^S} << 1 \quad \text{(S6)}$$

L: ratio of catalyst particle volume to the external surface area of the catalyst particle, which for spherical particles is given by Equation (S7):

$$L = \frac{V_p}{S_p} = \frac{\frac{4}{3} \cdot \pi \cdot r_p^3}{4 \cdot \pi \cdot r_p^2} = \frac{r_p}{3} = \frac{d_p}{6} \quad \text{(S7)}$$

D_i^e : effective diffusivity of the reactants inside the catalyst pores, calculated from Equation (S8):

$$D_i^e = \frac{D_M \cdot \varepsilon_p}{\tau} \quad \text{(S8)}$$

ε_p : porosity of catalyst particle; ϵ_p = 0,8

τ : catalyst particle tortuosity; τ = 6

C_i^S : concentration of the reagents on the catalyst surface.

As can be seen in Table S3, for both O_2 and VA the Weisz-Prater criterion is fulfilled, since for both reagents the value of $\Phi << 1$. It can thus be determined

that there are no limitations to matter transfer within the catalyst particle.

Table S3: Parameters inside the particle.

Parameter	Φ_{O2}	Φ_{VA}
Value	9.47×10^{-6}	4.67×10^{-5}

4 HPLC Method

In order to optimize the HPLC DAD method for VA and VN quantification, different mobile phases, column temperature and flow rates were tested.

First, a mobile phase that would allow an appropriate elution for both compounds was selected. To this end, different solutions of acetonitrile:water (30:70, 50:50), methanol:water (35:65, 50:50) and acetonitrile in an aqueous solution of 15% acetic acid were tested (Figure S1). The mobile phase acetonitrile:water 30:70 delivered the most defined peaks for both compounds with minimum baseline noise.

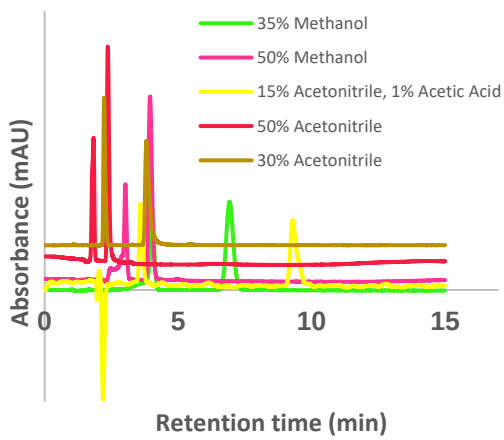

Figure S2: Chromatogram with different mobile phase.

Next, flow rate and column temperature were adjusted (Figure S2 and S3), with the purpose of minimizing retention times of the compounds, maintaining a good separation of the peaks. Two column temperatures were tested: 25 °C and 35 °C, resulting in no differences between chromatograms, therefore it was decided to select the lowest column temperature.

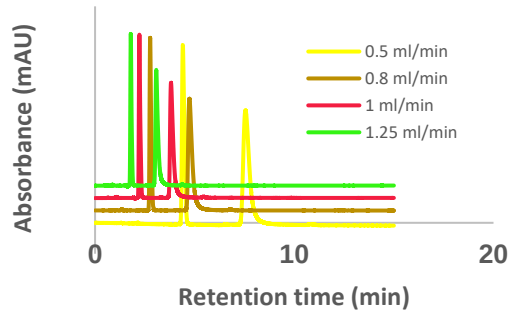

Figure S3: Chromatogram with different flow.

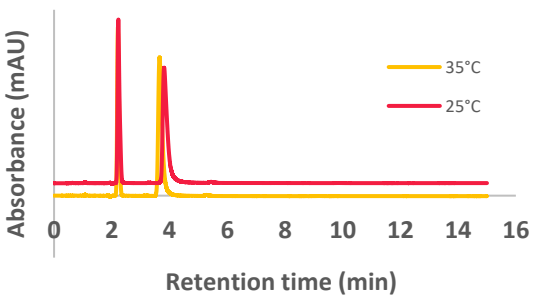

Figure S4: Chromatogram with different column temperature.

Regarding the flow rate, it was observed that at 1 mL/min, good peak resolution would be obtained with short run times, further increase in flow rate would lead to undesirable levels of pressure in the column.

Using the chromatographic conditions selected, the retention times for VA and VN were 2.2 minutes and 3.8 minutes respectively, and since the best response of the detector was observed at 230 nm, chromatograms at this wavelength were used for quantification (Figure S4).

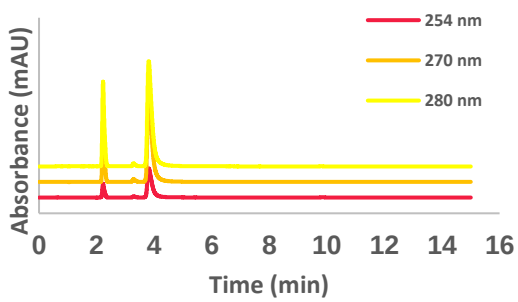

Figure S5: Chromatogram with different wavelength.

5 Products Identification by GC-MS

Samples from the reactions in which the selectivity to vanillin was low were analyzed by GC/MS. From the spectra, it was possible to identify, in addition to vanillyl alcohol and vanillin, some minor products: 2-methoxy-1,4 benzendiol, 1,4-2 methoxybenzoquinone as shown in Figure S5.

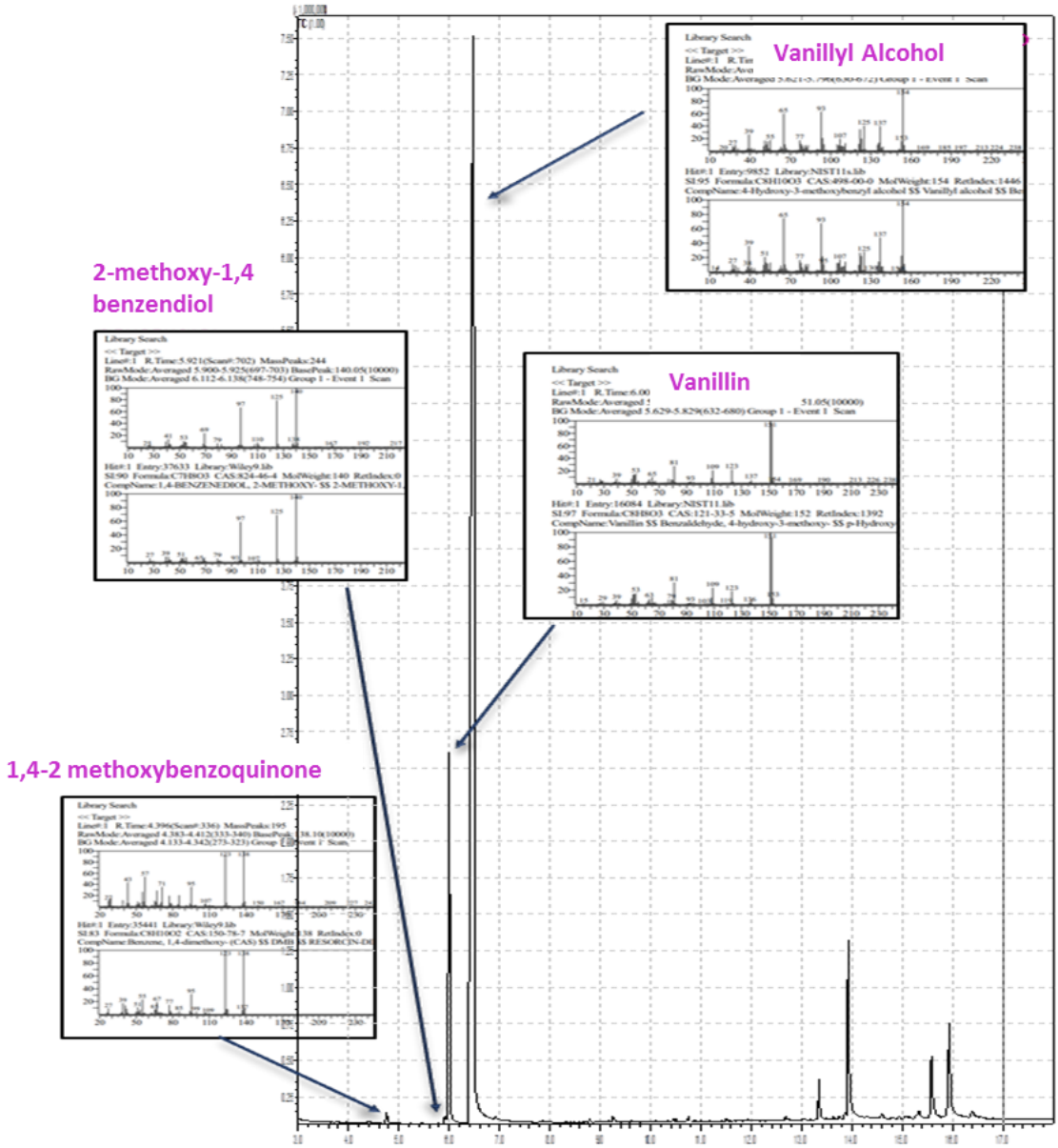

Figure S6: Chromatogram of an VA oxidation reaction sample, with the mass spectra of the identified compounds.